

DNA Cleavage on Photoexposure at the d–d Band in Ternary Copper(II) Complexes Using Red-Light Laser

Shanta Dhar, Munirathinam Nethaji, and Akhil R. Chakravarty*

Department of Inorganic & Physical Chemistry, Indian Institute of Science, Bangalore 560012, India

Received February 27, 2006

Ternary copper(II) complexes $[\text{Cu}(\text{L}^1)\text{B}](\text{ClO}_4)$ (**1**, **2**) and $[\text{Cu}(\text{L}^2)\text{B}](\text{ClO}_4)$ (**3**, **4**), where HL^1 and HL^2 are tridentate NSO- and ONO-donor Schiff bases and B is a heterocyclic base, viz. dipyrido[3,2-d:2',3'-f]quinoxaline (dpq, **1** and **3**) or dipyrido[3,2-a:2',3'-c]phenazine (dppz, **2** and **4**), were prepared and their DNA binding and photoinduced DNA cleavage activity studied. Complex **1**, structurally characterized by single-crystal X-ray crystallography, shows an axially elongated square-pyramidal (4 + 1) coordination geometry in which the monoanionic L^1 binds at the equatorial plane. The NN-donor dpq ligand exhibits an axial–equatorial binding mode. The complexes display good binding propensity to calf thymus DNA, giving a relative order **2** (NSO-dppz) > **4** (ONO-dppz) > **1** (NSO-dpq) > **3** (ONO-dpq). They cleave supercoiled pUC19 DNA to its nicked circular form when treated with 3-mercaptopropionic acid (MPA) by formation of hydroxyl radicals as the cleavage active species under dark reaction conditions. The photoinduced DNA cleavage activity of the complexes was investigated using UV radiation of 365 nm and red light of 633, 647.1, and 676.4 nm (CW He–Ne and Ar–Kr mixed gas ion laser sources) in the absence of MPA. Complexes **1** and **2**, having photoactive NSO-donor Schiff base and dpq/dppz ligands, show dual photosensitizing effects involving both the photoactive ligands in the ternary structure with significantly better cleavage properties when compared to those of **3** and **4**, having only photoactive dpq/dppz ligands. Involvement of singlet oxygen in the light-induced DNA cleavage reactions is proposed. A significant enhancement of the red-light-induced DNA cleavage activity is observed for the dpq and dppz complexes containing the sulfur ligand when compared to their earlier reported phen (1,10-phenanthroline) analogue. Enhancement of the cleavage activity on photoexposure at the d–d band indicates the occurrence of metal-assisted photosensitization processes involving the LMCT and d–d band in the ternary structure.

Introduction

Compounds exhibiting visible light-induced cleavage of double-stranded DNA are of current importance for their potential therapeutic applications.^{1–4} The photoexcited elec-

tronic state(s) of such compounds initiates a series of chemical reactions that lead to the oxidative cleavage of the nucleic acid. Porphyrin-based compounds like Photofrin and their analogues are known to exhibit red-light-induced photocleavage of DNA, and such compounds have found clinical applications in the emerging field of photodynamic therapy (PDT) of various cancers.^{5–10} Considering the skin

* To whom correspondence should be addressed. E-mail: arc@ipc.iisc.ernet.in.

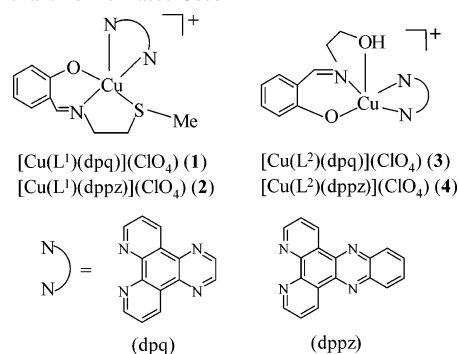
- (1) Chifotides, H. T.; Dunbar, K. R. *Acc. Chem. Res.* **2005**, *38*, 146. Szacilowski, K.; Macyk, W.; Drzewiecka-Matuszek, A.; Brindell, M.; Stochel, G. *Chem. Rev.* **2005**, *105*, 2647.
- (2) Armitage, B. *Chem. Rev.* **1998**, *98*, 1171.
- (3) Erkkila, K. E.; Odom, D. T.; Barton, J. K. *Chem. Rev.* **1999**, *99*, 2777. Pratiel, G.; Bernadou, J.; Meunier B. *Angew. Chem., Int. Ed. Engl.* **1995**, *34*, 746. Pogozelski, W. K.; Tullius, T. D. *Chem. Rev.* **1998**, *98*, 1089. McMillin, D. R.; McNett, K. M. *Chem. Rev.* **1998**, *98*, 1201. Metcalfe, C.; Thomas, J. A. *Chem. Soc. Rev.* **2003**, *32*, 215.
- (4) Kochevar, E.; Dunn, D. D. *Bioorganic Photochemistry*; Morrison, H., Ed.; John Wiley & Sons, New York, 1990; p 273. Karidi, K.; Garoufis, A.; Tsipis, A.; Hadjiliadis, N.; den Hulk, H.; Reedijk, J. *Dalton Trans.* **2005**, 1176. Lippard, S. J.; Berg, J. M. *Principles of Bioinorganic Chemistry*; University Science Books: Mill Valley, CA, 1994.

- (5) Canti, G.; De Simone, A.; Korbelik, M. *Photochem. Photobiol. Sci.* **2002**, *1*, 79. Dougherty, T. J.; Gomer, C. J.; Henderson, B. W.; Jori, G.; Kessel, D.; Korbelik, M.; Moan, J.; Peng, Q. *J. Natl. Cancer Inst.* **1998**, *90*, 889.
- (6) Clarke, M. J. *Coord. Chem. Rev.* **2003**, *236*, 209. Ali, H.; van Lier, J. E. *Chem. Rev.* **1999**, *99*, 2379.
- (7) Henderson, B. W.; Busch, T. M.; Vaughan, L. A.; Frawley, N. P.; Babich, D.; Sisa, T. A.; Zollo, J. D.; Dee, A. S.; Cooper, M. T.; Bellnier, D. A.; Greco, W. R.; Oseroff, A. R. *Cancer Res.* **2000**, *60*, 525.
- (8) De Rosa, M. C.; Crutchley, R. J. *Coord. Chem. Rev.* **2002**, *233–234*, 351. del C. Batle, A. M. *J. Photochem. Photobiol., B* **1993**, *20*, 5.

and hepatotoxicity¹¹ of porphyrin bases, there has been a recent surge in activities to search for non-porphyrinic organic and inorganic molecules suitable for PDT applications. Porphyrin-based drugs are not suitable for patients with porphyria or patients with known allergies to porphyrins. Bioactive organic molecules lacking any visible absorption bands within the “phototherapeutic window” are not suitable for PDT applications. Such compounds, often derived from the antitumor antibiotics or bioactive peptides and their conjugates, have moieties suitable for photoexcitations to the ³(n-π*) and/or ³(π-π*) state(s) at shorter wavelengths to display UV light-induced DNA cleavage activity.^{12–15} Among the transition-metal complexes, polypyridyl 4d- and 5d- metal complexes have been extensively studied for their photoinduced DNA cleavage activity, but such complexes are generally inactive in the “phototherapeutic window” of ca. 620–850 nm.^{16–20}

Transition-metal complexes are known to exhibit photoinduced DNA cleavage following different reaction pathways.²¹ We have shown that copper(II) complexes having photoactive and DNA binding ligands cleave DNA on irradiation with red light.^{22–26} Ternary mono-phen copper-

Scheme 1. Ternary Structures of the Copper(II) Complexes (1–4) and the Phenanthroline Bases Used



(II) complex $[\text{Cu}(\text{L}^1)(\text{phen})]^+$ having a NSO-donor Schiff base (L^1) efficiently cleaves DNA on exposure to red light by involving sulfur-to-copper charge transfer and a d–d band. Photoexposures at different wavelengths in the range of 600–700 nm show the highest DNA cleavage at the d–d band position, and we proposed metal-assisted d–d and LMCT band excitations for the photocleavage reactions.²⁶ To support our previous hypothesis, we have now explored this chemistry further by substituting the photoinactive phen ligand in $[\text{Cu}(\text{L}^1)(\text{phen})]^+$ with photoactive dipyridoquinoxaline (dpq) and dipyridophenazine (dppz) ligands as an additional photosensitizer to enhance the overall cleavage activity of the complexes involving the photoexcited ³(n-π*) and/or ³(π-π*) state(s) of the quinoxaline/phenazine moiety, and the results are presented here (Scheme 1).²⁷ We also prepared two ternary dpq and dppz complexes containing an ONO-donor Schiff base for control experiments. Herein, we report the synthesis, structure, DNA binding, and photoinduced DNA cleavage activity of $[\text{Cu}(\text{L}^1)\text{B}](\text{ClO}_4)$ (B = dpq (1), dppz, (2)) and $[\text{Cu}(\text{L}^2)\text{B}](\text{ClO}_4)$ (B = dpq (3), dppz (4)), where L^1 and L^2 are monoanionic tridentate NSO- and ONO-donor Schiff bases and B is dipyrido[3,2-d:2',3'-f]quinoxaline (dpq) or dipyrido[3,2-a:2',3'-c]phenazine (dppz). Significant results of this study are a different groove-binding preference of two phenanthroline bases, significant enhancement of red-light-induced DNA cleavage activity of complexes 1 and 2 in comparison to their phen analogue, and again observation of maximum cleavage activity on d–d band excitation. The importance of the metal in the ternary structure toward the photoexcitation processes is evidenced once again as the constituent Schiff base HL¹ and the phenanthroline bases *viz.* dpq and dppz alone do not show any apparent cleavage of DNA at red light.

Experimental Section

Materials and Measurements. All reagents and chemicals were procured from commercial sources (SD Fine Chemicals, India;

- (9) Sternberg, E. D.; Dolphin, D.; Brückner, C. *Tetrahedron* **1998**, *54*, 4151.
- (10) Dougherty, T. J.; Gomer, C. J.; Henderson, B. W.; Jori, G.; Kessel, D.; Korbelik, M.; Moan, J.; Peng, Q. *J. Natl. Cancer Inst.* **1998**, *90*, 889. Sessler, J. L.; Hemmi, G.; Mody, T. D.; Murai, T.; Burrell, A.; Young, S. W. *Acc. Chem. Res.* **1994**, *27*, 43.
- (11) Ochsner, M. J. *Photochem. Photobiol.*, **B** **1996**, *32*, 3.
- (12) Gillman, I. G.; Yezek, J. M.; Manderville, R. A. *Chem. Commun.* **1998**, 647. Frier, C.; Mouscadet, J. F.; Decout, J. L.; Auclair, C.; Fontecave, M. *Chem. Commun.* **1998**, 2457.
- (13) Theodorakis, E. A.; Xiang, X.; Blom, P. *Chem. Commun.* **1997**, 1463. Qian, X.; Huang, T.-B.; Wei, D.; Zhu, D.-H.; Fan, M.; Yao, W. *J. Chem. Soc., Perkin Trans. 2* **2000**, 715.
- (14) Toshima, K.; Takai, S.; Maeda, Y.; Takano, R.; Matsumura, S. *Angew. Chem., Int. Ed.* **2000**, *39*, 3656. Schmittel, M.; Viola, G.; Dall'Acqua, F.; Morbach, G. *Chem. Commun.* **2003**, 646. Breslin, D. T.; Coury, J. E.; Anderson, J. R.; McFail-Isom, L.; Kan, Y.; Williams, L. D.; Bottomley, L. A.; Schuster, G. B. *J. Am. Chem. Soc.* **1997**, *119*, 5043.
- (15) Mahon, K. P.; Rodrigo, J. F.; Meoz, O.; Prestwich, E. G.; Kelley, S. O. *Chem. Commun.* **2003**, 1956. Kovalenko, S. V.; Alabugin, I. V. *Chem. Commun.* **2005**, 1444. Bohne, C.; Faulhaber, K.; Giese, B.; Häfner, A.; Hofmann, A.; Ihmels, H.; Köhler, A.-K.; Perä, S.; Schneider, F.; Sheepwash, M. A. L. *J. Am. Chem. Soc.* **2005**, *127*, 76.
- (16) Bohne, C.; Faulhaber, K.; Giese, B.; Häfner, A.; Hofmann, A.; Ihmels, H.; Köhler, A.-K.; Perä, S.; Schneider, F.; Sheepwash, M. A. L. *J. Am. Chem. Soc.* **2005**, *127*, 76. Chow, C. S.; Barton, J. K. *Methods Enzymol.* **1992**, *212*, 219.
- (17) Kalsbeck, W. A.; Gingell, D. M.; Malinsky, J. E.; Thorp, H. H. *Inorg. Chem.* **1994**, *33*, 3313. Mei, H.-Y.; Barton, J. K. *Proc. Natl. Acad. Sci. U.S.A.* **1988**, *85*, 1339. Sentagne, C.; Chambron, J.-C.; Sauvage, J.-P.; Paillous, N. *J. Photochem. Photobiol.*, **B** **1994**, *26*, 165.
- (18) Lecomte, J.-P.; Kirsch-De Mesmaeker, A.; Feeny, M. M.; Kelly, J. M. *Inorg. Chem.* **1995**, *34*, 6481. Lecomte, J.-P.; Kirsch-De Mesmaeker, A.; Kelly, J. M.; Tossi, A. B.; Gerner, H. *Photochem. Photobiol.* **1992**, *55*, 681. Tossi, A. B.; Kelly, J. M. *Photochem. Photobiol.* **1989**, *49*, 545.
- (19) Bradley, P. M.; Angeles-Boza, A. M.; Dunbar, K. R.; Turro, C. *Inorg. Chem.* **2004**, *43*, 2450. Angeles-Boza, A. M.; Bradley, P. M.; Fu, P. K.-L.; Wicke, S. E.; Bacsa, J.; Dunbar, K. R.; Turro, C. *Inorg. Chem.* **2004**, *43*, 8510.
- (20) Phillips, T.; Haq, I.; Meijer, A. J. H. M.; Adams, H.; Soutar, I.; Swanson, L.; Sykes, M. J.; Thomas, J. A. *Biochemistry* **2004**, *43*, 13657. Maurer, T. D.; Kraft, B. J.; Lato, S. M.; Ellington, A. D.; Zaleski, J. M. *Chem. Commun.* **2000**, 69.
- (21) Burrows, C. J.; Muller, J. G. *Chem. Rev.* **1998**, *98*, 1109.
- (22) Dhar, S.; Nethaji, M.; Chakravarty, A. R. *Inorg. Chem.* **2005**, *44*, 8876.
- (23) Dhar, S.; Senapati, D.; Reddy, P. A. N.; Das, P. K.; Chakravarty, A. R. *Chem. Commun.* **2003**, 2452.

- (24) Dhar, S.; Nethaji, M.; Chakravarty, A. R. *Dalton Trans.* **2005**, 344. Dhar, S.; Nethaji, M.; Chakravarty, A. R. *J. Inorg. Biochem.* **2005**, *99*, 805. Dhar, S.; Nethaji, M.; Chakravarty, A. R. *Inorg. Chim. Acta* **2005**, *358*, 2437.
- (25) Dhar, S.; Chakravarty, A. R. *Inorg. Chem.* **2005**, *44*, 2582.
- (26) Dhar, S.; Chakravarty, A. R. *Inorg. Chem.* **2003**, *42*, 2483; Dhar, S.; Senapati, D.; Das, P. K.; Chattopadhyay, P.; Nethaji, M.; Chakravarty, A. R. *J. Am. Chem. Soc.* **2003**, *125*, 12118.
- (27) Toshima, K.; Takano, R.; Ozawa, T.; Matsumura, S. *Chem. Commun.* **2002**, 212.

Aldrich, USA) and used without further purification. Solvents used were purified by standard procedures.²⁸ Supercoiled pUC19 DNA (cesium chloride purified) was purchased from Bangalore Genie (India). Tris(hydroxymethyl)aminomethane–HCl (Tris–HCl) buffer solution was prepared using deionized and sonicated triple-distilled water. Calf thymus DNA, agarose (molecular biology grade), distamycin, catalase, superoxide dismutase (SOD), and ethidium bromide (EB) were from Sigma (USA).

Elemental analyses were done using a Thermo Finnigan Flash EA 1112 CHNSO analyzer. The infrared, electronic, and fluorescence spectral data were obtained from Perkin-Elmer Spectrum One FTIR, Perkin-Elmer Lambda 35 UV–vis, and Perkin-Elmer LS-50B spectrophotometers, respectively. Electrochemical measurements were performed at 25 °C on an EG&G PAR model 253 VersaStat potentiostat/galvanostat with electrochemical analysis software 270 for cyclic voltammetric work using a three-electrode setup consisting of glassy carbon working, platinum wire auxiliary, and saturated calomel reference electrodes. Magnetic susceptibility data at 298 K were obtained for polycrystalline samples using a George Associates Inc. Lewis-coil-force magnetometer system (Berkeley, CA).

Preparation of [Cu(LⁿB)(ClO₄) (n = 1, B = dpq (1) and dppz (2); n = 2, B = dpq (3) and dppz (4)). Complexes 1–4 were prepared by a general procedure in which a 0.2 g (0.5 mmol) quantity of dimeric copper(II) acetate hydrate in 15 mL of methanol was reacted with the heterocyclic base (0.8 mmol, 0.19 g of dpq; 0.23 g of dppz) while stirring at 25 °C for 0.5 h followed by addition of the respective Schiff base (1.2 mmol, 0.24 g of HL¹; 0.19 g of HL²) taken in 10 mL of MeOH. The reaction mixture was stirred for 1 h, and the product was isolated as a green solid in ~75% yield on addition of a methanolic solution of NaClO₄ (1.0 mmol, 0.12 g). The solid was isolated, washed with cold methanol, and finally dried in vacuo over P₄O₁₀. All complexes were obtained in crystalline form on slow evaporation of their respective methanol solution. Anal. Calcd for C₂₄H₂₀N₅O₅SClCu (1): C, 48.89; H, 3.39; N, 11.88. Found: C, 48.61; H, 3.67; N, 11.60. FTIR, cm⁻¹ (KBr phase; br, broad; vs, very strong; s, strong; m, medium; w, weak): 3440br, 1628s, 1522m, 1449m, 1405m, 1385m, 1315w, 1212w, 1099vs, 772w, 733m, 619m, 439w. UV–vis in MeCN [λ_{\max} , nm (ϵ , M⁻¹ cm⁻¹): 654 (150), 480 (140), 401 (760), 257 (85 000), 224 (60 000). Magnetic data (μ_{eff} at 298 K): 1.91 μ_{B} . Anal. Calcd for C₂₈H₂₂N₅O₅SClCu (2): C, 52.58; H, 3.44; N, 10.95. Found: C, 52.39; H, 3.67; N, 10.74. FTIR, cm⁻¹ (KBr phase): 3420br, 1615s, 1495m, 1419m, 1355w, 1089vs, 762m, 736m, 623m, 423w. UV–vis in MeCN [λ_{\max} , nm (ϵ , M⁻¹ cm⁻¹): 645 (120), 397 (1520), 397 (1500), 376 (9850), 357 (9500), 275 (38 400). Magnetic data (μ_{eff} at 298 K): 1.75 μ_{B} . Anal. Calcd for C₂₃H₁₈N₅O₆ClCu (3): C, 49.37; H, 3.22; N, 12.52. Found: C, 49.19; H, 3.42; N, 12.69. FTIR, cm⁻¹ (KBr phase): 3443br, 1608s, 1525m, 1439m, 1412w, 1379w, 1342w, 1122vs, 906w, 766w, 726w, 619w, 439w. UV–vis in MeCN [λ_{\max} , nm (ϵ , M⁻¹ cm⁻¹): 628 (150), 410 (1550), 255 (69 700), 219 (43 600). Magnetic data (μ_{eff} at 298 K): 1.82 μ_{B} . Anal. Calcd for C₂₇H₂₀N₅O₆ClCu (4): C, 53.20; H, 3.28; N, 11.50. Found: C, 53.13; H, 3.35; N, 11.31. FTIR, cm⁻¹ (KBr phase): 3440br, 1615s, 1565m, 1419m, 1355w, 1096vs, 759m, 735s, 426w. UV–vis in MeCN [λ_{\max} , nm (ϵ , M⁻¹ cm⁻¹): 611 (115), 375 (5000), 275 (80 300). Magnetic data (μ_{eff} at 298 K): 1.92 μ_{B} .

Solubility and Stability. The complexes are moderately soluble in common organic solvents like MeCN, CH₂Cl₂, DMF, and MeOH, less soluble in water, and insoluble in hydrocarbons. They are stable

Table 1. Selected Crystallographic Data for the Complex [Cu(L¹)(dpq)](ClO₄) (1)

chemical formula	C ₂₄ H ₂₀ ClCuN ₅ O ₅ S
fw (g mol ⁻¹)	589.50
space group	P $\bar{1}$
a (Å)	12.209(7)
b (Å)	13.737(8)
c (Å)	14.884(9)
α (deg)	79.304(11)
β (deg)	83.491(11)
γ (deg)	89.745(12)
V (Å ³)	2437(2)
Z	4
T (K)	293(2)
ρ_{calcd} (g cm ⁻³)	1.607
λ (Mo K α) (Å)	0.71073
μ (cm ⁻¹)	11.39
R (F _o) ^a [R all data]	0.0909 [0.1419]
wR (F _o) ^b [wR (all data)]	0.1733 [0.1941]

^a $R = \sum ||F_o| - |F_c|| / \sum |F_o|$. ^b $wR = [\sum w(|F_o| - |F_c|)^2 / \sum w|F_o|^2]^{1/2}$, where $w = 1/[\sigma^2(F_o^2) + (AP)^2 + BP]$, where $\rho = [\text{Max}(F_o^2, 0) + 2F_c^2]/3$. A and B values are 0.0848 and 0.0000, respectively.

in the solid as well as in the solution phase. *Caution!* Perchlorate salts of metal complexes are potentially explosive, and only a small quantity of the sample was used with necessary precautions.

X-ray Crystallographic Procedures. Single crystals of 1 were grown on slow evaporation of a methanol solution of the complex. A crystal of 0.23 × 0.11 × 0.09 mm size was mounted on a glass fiber using epoxy cement. X-ray diffraction data were measured in frames with increasing ω (width of 0.3° per frame) at a scan speed of 20 s per frame using a Bruker SMART APEX CCD diffractometer, equipped with a fine focus sealed tube Mo K α X-ray source. SMART software was used for data acquisition and SAINT for data extraction. Empirical absorption corrections were made on the intensity data.²⁹ The structure was solved and refined using the SHELX system of programs.³⁰ Non-hydrogen atoms were refined anisotropically. Hydrogen atoms belonging to the complex were in a fixed position and refined using a riding model. The structure was refined with a goodness-of-fit (GoF) value of 1.132. The maximum shift/esd value and the highest peak in the final difference Fourier map were 0.0 and 0.94 e Å⁻³, respectively. Selected crystallographic data are given in Table 1. The perspective view of the cationic complex was obtained using the ORTEP program.³¹

DNA Binding Studies. The fluorescence spectral method using ethidium bromide (EB) as a reference was used to determine the relative DNA binding properties of the complexes to calf thymus (CT) DNA in Tris–HCl/NaCl buffer (5 mM, pH 7.2). DNA concentrations, expressed with respect to mononucleotides, were determined spectrophotometrically using the reported data for a molar absorption coefficient of 6600 M⁻¹ cm⁻¹ at 260 nm.³² Fluorescence intensities of EB at 601 nm with an excitation wavelength of 510 nm were measured at different complex concentrations. Reduction in the emission intensity was observed with addition of the complexes. The relative binding tendency of the complexes to CT DNA was determined from a comparison of the slopes of the lines in the fluorescence intensity versus complex concentration plot. The apparent binding constant (K_{app}) was

(29) Walker, N.; Stuart, D. *Acta Crystallogr.* **1993**, A39, 158.

(30) Sheldrick, G. M. *SHELX-97, Programs for Crystal Structure Solution and Refinement*; University of Göttingen: Göttingen, Germany, 1997.

(31) Johnson, C. K. *ORTEP, Report ORNL-5138*; Oak Ridge National Laboratory: Oak Ridge, TN, 1976.

(32) Reichmann, M. E.; Rice, S. A.; Thomas, C. A.; Doty, P. *J. Am. Chem. Soc.* **1954**, 76, 3047.

(28) Perrin, D. D.; Armarego, W. L. F.; Perrin, D. R. *Purification of Laboratory Chemicals*; Pergamon Press: Oxford, 1980.

Table 2. Physicochemical Data for the Complexes 1–4

complex	IR ^a , cm ⁻¹ ν(C=N), ν(CIO ₄)	λ, nm (ε, M ⁻¹ cm ⁻¹) ^b d–d band	E _{1/2} , V (ΔE _p , mV) ^c	K _b , ^d M ⁻¹
[Cu(L ¹)(dpq)](ClO ₄) (1)	1628, 1099	654 (150)	-0.10 (300)	1.2 × 10 ⁴
[Cu(L ¹)(dppz)](ClO ₄) (2)	1615, 1089	645 (120)	0.07 (210)	4.6 × 10 ⁴
[Cu(L ²)(dpq)](ClO ₄) (3)	1608, 1122	628 (150)	-0.09 (340)	0.9 × 10 ⁴
[Cu(L ²)(dppz)](ClO ₄) (4)	1615, 1096	611 (115)	0.08 (190)	3.3 × 10 ⁴

^a In KBr phase. ^b In DMF–Tris buffer. ^c Cu(II)/Cu(I) couple at a scan rate of 50 mV s⁻¹ in DMF–Tris buffer (1:4 v/v)/0.1 M KCl. E_{1/2} = 0.5(E_{pa} + E_{pc}). ΔE_p = E_{pa} – E_{pc}, where E_{pa} and E_{pc} are anodic and cathodic peak potentials, respectively. ^d DNA binding constant.

calculated using the equation $K_{EB}[EB] = K_{app}[\text{complex}]$, where the complex concentration was the value at a 50% reduction of the fluorescence intensity of EB and $K_{EB} = 1.0 \times 10^7 \text{ M}^{-1}$ ([EB] = 1.3 μM).³³ The absorption spectral titration method was used to determine the binding constants (K_b) of the complexes using the expression $[\text{DNA}]/(\epsilon_a - \epsilon_f) = [\text{DNA}]/(\epsilon_b - \epsilon_f) + 1/K_b(\epsilon_b - \epsilon_f)$, where ϵ_a , ϵ_f , and ϵ_b are the apparent absorption coefficient, ϵ of the complex in free form, and ϵ of the complex in fully bound form, respectively. The K_b value was obtained from the $[\text{DNA}]/(\epsilon_a - \epsilon_f)$ vs $[\text{DNA}]$ plot.³⁴

Light Sources for DNA Photocleavage. A monochromatic 12 W UV lamp of 365 nm (Bangalore Genie; sample area of illumination, 45 mm²) was used for irradiation in the UV region. For visible light irradiations, we used a He–Ne CW Laser (Research Electro-Optics Inc.) of 633 nm (12 mW; beam diameter, 0.88 mm; beam divergence, 0.92 mrad) and a Spectra Physics Water-Cooled Mixed-Gas Ion Laser Stabilite 2018-RM (beam diameter at 1/e² 1.8 mm ± 10% and beam divergence with full angle 0.70 mrad ± 10%) laser at 647.1 and 676.4 nm. The power of the laser beam was 100 mW, measured using a Spectra Physics CW Laser Power Meter (model 407A).

DNA Cleavage Experiments. The extent of photoinduced cleavage of supercoiled (SC) pUC19 DNA by the complexes was studied by agarose gel electrophoresis. Under aerobic reaction conditions, each pUC19 DNA sample (1 μL, 0.2 μg, 33 μM) in 50 mM Tris-HCl buffer (pH, 7.2; ionic strength, 25 mM) containing 50 mM NaCl was irradiated in the presence of the complex under examination of varied concentrations. Eppendorf and glass vials were used for the UV and visible light experiments, respectively, in a dark room at 25 °C. After photoexposure, the samples were incubated for 1 h at 37 °C followed by addition to the loading buffer containing 25% bromophenol blue, 0.25% xylene cyanol, and 30% glycerol (3 μL), and the solution was finally loaded on 0.8% agarose gel containing 1.0 μg/mL ethidium bromide. Electrophoresis was carried out in a dark chamber for 3 h at 40 V in TAE (Tris-acetate-EDTA) buffer. DNA bands were detected under UV radiation with a UV transilluminator (UVITEC, 312 nm). Photographs were taken with a UVITEC CCD video camera, and quantification of the bands was achieved by UViband 1D gel analysis software. Corrections were made to the data for the low level of nicked circular (NC) form present in the original SC DNA sample and for the low affinity of EB binding to SC compared to NC form of DNA.³⁵ Several experiments were carried out in the presence of different additives for mechanistic insights of the DNA photocleavage reactions. These reactions were done by adding reagents to SC DNA prior to addition of the complex before photoirradiation.

DNA cleavage experiments were also carried out using 3-mercaptopropionic acid (MPA) as a reducing agent under dark reaction conditions and to determine the groove binding preference of the

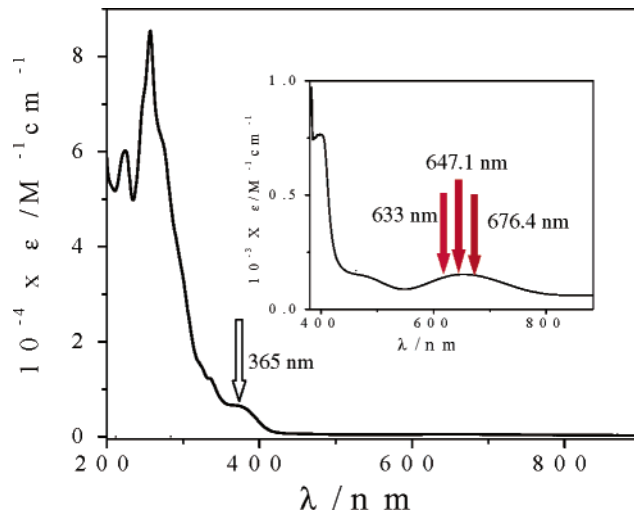


Figure 1. Electronic spectrum of [Cu(L¹)(dpq)](ClO₄) (**1**) in MeCN showing different wavelengths used for photoirradiations (arrow).

complexes in the presence of distamycin.³⁶ Supercoiled pUC19 DNA (0.2 μg; 33 μM) in 50 mM Tris-HCl buffer (pH, 7.2) containing 50 mM NaCl was treated with the metal complex (40 μM) and MPA (5 mM) followed by dilution with the Tris-HCl buffer to a total volume of 18 μL. Samples were incubated for 1 h at 37 °C in dark. The concentrations of the complexes or additives in all DNA cleavage experiments corresponded to the quantity of the sample in 2 μL of stock solution (complex in 2 μL DMF) used prior to dilution to the 18 μL final volume with Tris-HCl buffer.

Results and Discussion

General and Structural Aspects. We synthesized two new copper(II) complexes (**1** and **2**) having photoactive NSO-donor Schiff base and photoactive phenanthroline bases with quinoxaline/phenazine moieties to provide further evidence to support our previous observation of the involvement of the LMCT and d–d band in the metal-assisted DNA photocleavage activity of [Cu(L¹)(phen)]⁺ having the same Schiff base ligand (Scheme 1).²⁶ For a comparative study related to the role of sulfur in the photocleavage reaction and to explore the extent of the contribution arising from the ONS-donor ligand toward DNA photocleavage activity, we prepared the ternary complexes **3** and **4** containing photoinactive ONO-donor Schiff base. Complexes **1–4** were characterized from the analytical and physicochemical data (Table 2). They exhibit a d–d band in the range of 610–660 nm in the electronic spectra (Figure 1). The bands near 400 nm are assignable to the ligand to copper(II) charge

(33) Lee, M.; Rhodes, A. L.; Wyatt, M. D.; Forrow, S.; Hartley, J. A. *Biochemistry* **1993**, *28*, 7268.

(34) Wolf, A.; Shimer, G. H., Jr.; Meehan, T. *Biochemistry* **1987**, *26*, 6392.

(35) Bernadou, J.; Pratiel, G.; Bennis, F.; Girardet, M.; Meunier, B. *Biochemistry* **1989**, *28*, 7268.

(36) Dhar, S.; Reddy, P. A. N.; Nethaji, M.; Mahadevan, S.; Saha, M. K.; Chakravarty, A. R. *Inorg. Chem.* **2002**, *41*, 3469.

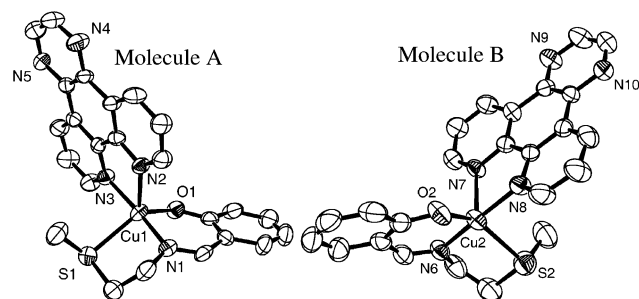


Figure 2. ORTEP views of two independent molecules of $[\text{Cu}(\text{L}^1)(\text{dpq})](\text{ClO}_4)$ (**1**) showing atom labeling for the metal and heteroatoms and 50% probability thermal ellipsoids.

Table 3. Selected Bond Distances (Å) and Angles (deg) for $[\text{Cu}(\text{L}^1)(\text{dpq})](\text{ClO}_4)$ (**1**) with esd's in the Parenthesis

molecule A		molecule B	
Cu(1)–O(1)	1.935(4)	Cu(2)–O(2)	1.916(5)
Cu(1)–N(1)	1.935(5)	Cu(2)–N(6)	1.944(5)
Cu(1)–N(2)	2.164(5)	Cu(2)–N(7)	2.193(6)
Cu(1)–N(3)	2.015(5)	Cu(2)–N(8)	2.019(5)
Cu(1)–S(1)	2.431(2)	Cu(2)–S(2)	2.434(3)
N(1)–Cu(1)–O(1)	93.3(2)	N(6)–Cu(2)–O(2)	94.7(2)
N(1)–Cu(1)–N(2)	96.3(2)	N(6)–Cu(2)–N(7)	96.9(2)
N(2)–Cu(1)–O(1)	113.69(19)	N(7)–Cu(2)–O(2)	111.2(2)
N(1)–Cu(1)–N(3)	172.1(2)	N(6)–Cu(2)–N(8)	172.1(2)
N(3)–Cu(1)–O(1)	94.4(2)	N(8)–Cu(2)–O(2)	92.8(2)
N(2)–Cu(1)–N(3)	79.5(2)	N(7)–Cu(2)–N(8)	78.0(2)
N(1)–Cu(1)–S(1)	84.67(17)	N(6)–Cu(2)–S(2)	84.43(18)
O(1)–Cu(1)–S(1)	131.48(15)	O(2)–Cu(2)–S(2)	143.08(18)
N(2)–Cu(1)–S(1)	114.71(15)	N(7)–Cu(2)–S(2)	105.55(16)
N(3)–Cu(1)–S(1)	91.06(15)	N(8)–Cu(2)–S(2)	91.16(18)

transfer (LMCT) transitions.³⁷ The redox-active dpq and dpdz complexes show cyclic voltammograms assignable to the Cu(II)/Cu(I) couple near -0.1 and 0.07 V (vs SCE), respectively, in DMF-Tris buffer medium (Figure S1).^{38,39} As expected, the dpdz ligand with its phenazine moiety stabilizes the copper(I) state more than the dpq ligand with a quinoxaline ring.

Complex **1** has been structurally characterized by X-ray crystallography (Figure 2). Selected bond distances and bond angles data are presented in Table 3. The crystal structure shows the presence of two discrete monomeric cationic complexes and two lattice perchlorate anions in the crystallographic asymmetric unit of the triclinic crystal system in *P1* space group. These two molecules show different trigonality parameter (τ) values of 0.68 and 0.48, possibly due to the crystal packing effect ($\tau = 0.0$ for idealized square-pyramidal and 1.0 for trigonal-bipyramidal geometry).⁴⁰ Each complex has the metal bound to a tridentate NSO-donor Schiff base at the equatorial plane, and the bidentate dpq ligand displays axial–equatorial bonding in the distorted square-pyramidal ($4 + 1$) CuN_3OS coordination geometry. The average Cu–O and Cu–S bond distances are 1.92 and 2.43 Å, respectively. The average Cu–N_(axial) bond distance

is 2.1 Å. The structural features of the dpq complex **1** are similar to those reported for its phen analogue.²⁶ The crystal structure of the complex shows intermolecular hydrogen-bonding interactions involving the complex and the lattice perchlorate anion (Figure S2). The structural features of **1** and **2**, however, differ from those of **3** and **4** (Scheme 1). The structure proposed for complexes **3** and **4** with an axial–equatorial binding ONO-donor ligand is based on the reported crystal structure of their phen analogue.²⁶

DNA Binding Properties. Spectral techniques have been used to determine the mode and propensity of the binding of the complexes to calf thymus (CT) DNA (Figures S3 and S4). The relative binding of the complexes to calf thymus DNA has been studied by the fluorescence method using the emission intensity of ethidium bromide (EB). Ethidium bromide alone or in the presence of the metal complex does not show any emission intensity in Tris buffer medium due to fluorescence quenching of the free EB by the solvent molecules (Figure S3).⁴¹ In presence of DNA, EB shows enhanced emission intensity due to its intercalative binding to DNA. A competitive binding of the copper complex having planar phenanthroline base to calf thymus DNA is expected to either displace the bound EB or quench EB fluorescence due to the close proximity of paramagnetic copper(II) species to the DNA-bound EB. As a consequence, the emission intensity of EB is likely to decrease. The observed binding propensity of **1–4** follows the order **2** (ONS-dppz) > **4** (ONO-dppz) > **1** (ONS-dpq) > **3** (ONO-dpq). All these complexes show significantly better DNA binding than their reported ternary mono-phen analogue $[\text{Cu}(\text{L}^1)(\text{phen})](\text{ClO}_4)$.²⁶ The apparent binding constant (K_{app}) values for **1–4** are found to be 4.6×10^5 , 5.7×10^6 , 1.8×10^5 , and 4.0×10^6 M^{-1} , respectively.

We determined the binding constants of the complexes to CT DNA by monitoring the change of intensity of the CT spectral bands on increasing the concentration of CT DNA. All four complexes show a minor bathochromic shift of ca. 2–5 nm along with hypochromicity in the range of 40–45%. The K_b values obtained for **1–4** by absorption spectral method are 1.8×10^4 , 4.6×10^4 , 0.9×10^4 , and 3.3×10^4 M^{-1} , respectively. The binding order is the same as that observed by the fluorescence spectral method.

Chemical Nuclease Activity. The DNA cleavage activity of the complexes has been studied using a plasmid relaxation assay to monitor the conversion of circular supercoiled DNA (SC) to its nicked circular (NC) form. All complexes are inactive in the absence of any reducing agent when the reactions are carried out in the dark. In the presence of 3-mercaptopropionic acid (5 mM) as a reducing agent, the complexes (40 μM) show efficient DNA cleavage activity giving the order **2** (NSO-dppz) > **4** (ONO-dppz) > **1** (NSO-dpq) > **3** (ONO-dpq) (Figure S5).

Control experiments were done to determine the groove selectivity of the complexes and for mechanistic insights. Addition of minor-groove binder distamycin to SC DNA

(37) Kita, T.; Miura, I.; Nakayama, N.; Kawata, T.; Kano, K.; Hirota, S.; Koderu, M. *J. Am. Chem. Soc.* **2001**, *123*, 7715.

(38) Santra, B. K.; Reddy, P. A. N.; Nethaji, M.; Chakravarty, A. R. *Inorg. Chem.* **2002**, *41*, 1328.

(39) Santra, B. K.; Reddy, P. A. N.; Nethaji, M.; Chakravarty, A. R. *J. Chem. Soc., Dalton Trans.* **2001**, 3553.

(40) Addison, A. W.; Rao, T. N.; Reedijk, J.; Rijn, J. V.; Verschoor, G. C. *J. Chem. Soc., Dalton Trans.* **1984**, 1349.

(41) Waring, M. J. *J. Mol. Biol.* **1965**, *13*, 269. Le Pecq, J.-B.; Paoletti, C. *J. Mol. Biol.* **1967**, *27*, 87.

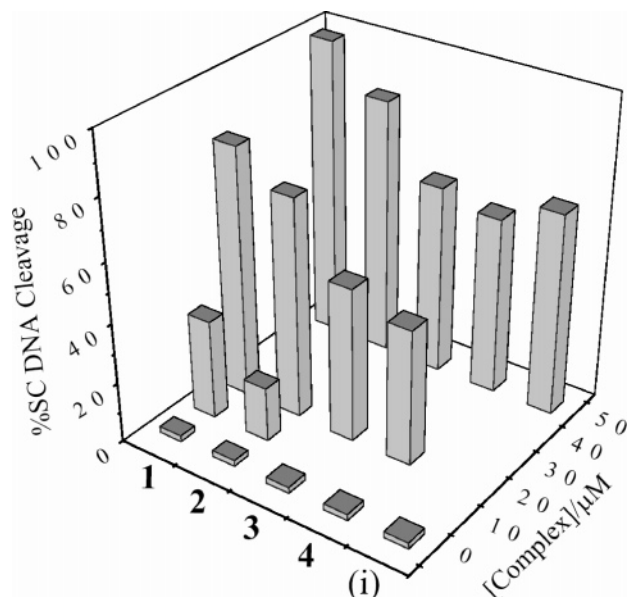


Figure 3. Photoinduced cleavage of SC pUC19 DNA (0.2 μg, 33 μM) by complexes **1–4** and [Cu(L¹)(phen)](ClO₄) (**i**) in 50 mM Tris-HCl/NaCl buffer (pH, 7.2) containing DMF (10%) with different complex concentrations using monochromatic UV radiation of 365 nm (12 W) for an exposure time of 30 min.

inhibits cleavage for the dpq complexes, while the dppz complexes remain cleavage active. The results suggest minor- and major-groove binding preferences for the dpq and dppz complexes, respectively.³⁶ Addition of hydroxyl radical scavenger DMSO results in complete inhibition of the cleavage activity for all complexes, suggesting the possibility of formation of diffusible hydroxyl radical as the reactive species leading to strand scission.⁴²

Photoinduced DNA Cleavage Activity. The DNA photocleavage activity of the complexes **1–4** has been studied by irradiating the complexes under aerobic conditions in buffered aqueous solutions in the presence of SC pUC19 DNA with both UV and visible (red) lights. The extent of DNA cleavage was determined by agarose-gel electrophoresis. The complexes are cleavage inactive in the dark in the absence of any external reagents. They show cleavage of SC DNA to its NC form on exposure to UV light of 365 nm (Figure 3 and Figure S6). The cleavage efficiency follows the order **1** (NSO-dpq) > **2** (NSO-dppz) > **3** (ONO-dpq) > **4** (ONO-dppz). Complexes **1** and **2** contain both photoactive NSO-donor Schiff base and the phenanthroline bases. The enhanced photonuclease activity of **1** and **2** is due to the photosensitization ability of both ligands in the ternary structure in comparison to that observed for [Cu(L¹)(phen)](ClO₄) having the photoinactive phen ligand.²⁶ The photocleavage activity of the complexes having the NSO-donor Schiff base (L¹) is significantly higher than those having the photoinactive ONO-donor Schiff base (L²). Control experiments using dpq and dppz ligand alone with their photoexcited ³(n-π*) and/or ³(π-π*) state(s) show no apparent

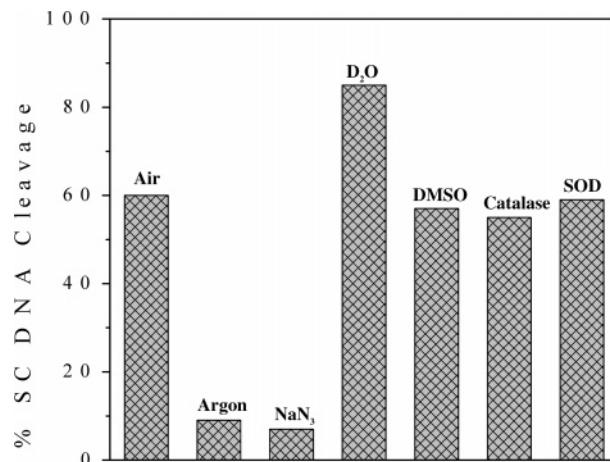


Figure 4. Bar diagram showing the cleavage of SC pUC19 DNA (0.2 μg, 33 μM) by **1** (50 μM) in the presence of different additives on photoirradiation at 365 nm for 10 min exposure time in 50 mM Tris-HCl/NaCl buffer (pH 7.2) containing DMF (10%). The additives used are as follows: NaN₃, 100 μM; D₂O, 14 μL; DMSO, 2 μL; SOD, 2000 UI/mL; catalase, 2000 UI/mL.

cleavage of DNA at 365 nm under similar experimental conditions. The same ligand when bound to copper(II) as in complexes **3** and **4** exhibits significant DNA cleavage. The mediatory role of the metal ion (Cu²⁺) in the photoexcitation process is evident from the DNA cleavage data.^{22–26} The reduced cleavage efficiency of the dppz complexes compared to those having dpq ligand with a quinoxaline moiety could be due to the presence of an additional aromatic ring in the phenazine moiety.⁴³

Complexes **1–4** are cleavage inactive under argon atmosphere, indicating the possibility of involvement of some reactive oxygen species in the DNA cleavage reactions (Figure 4). To explore the mechanistic aspects of the cleavage reaction, a series of control experiments were carried out using external reagents like superoxide dismutase⁴⁴ (SOD 2000 UI/mL), catalase (2000 UI/mL as scavenger of O₂^{•-} and H₂O₂), DMSO (2 μL as OH• radical scavenger), and NaN₃⁴⁵ (100 μM as singlet oxygen quencher) (Figure 4). The reactions were also carried out in deuterated water (D₂O, 14 μL) in which the lifetime of singlet oxygen is known to be significantly higher than that in water.⁴⁶ We have not observed any significant inhibition of DNA photocleavage on addition of SOD or catalase, indicating the noninvolvement of superoxide or hydroxyl radicals in the DNA cleavage. DMSO addition shows no apparent effect on the cleavage activity, thus excluding the possibility of hydroxyl radical formation. In contrast, complete inhibition and increase of strand breaks are observed in the presence of NaN₃ and deuterated buffer, respectively, suggesting formation of singlet oxygen (O₂, ¹Δ_g) as the key intermediate in the DNA photocleavage induced by complexes **1–4**.

(43) Gupta, T.; Dhar, S.; Nethaji, M.; Chakravarty, A. R. *Dalton Trans.* **2004**, 1896.

(44) Baudoin, O.; Teulade-Fichou, M.-P.; Vigneron, J.-P.; Lehn, J.-M. *Chem. Commun.* **1998**, 2349.

(45) Foote, C. S.; Fujimoto, T. T.; Chang, Y. C. *Tetrahedron Lett.* **1972**, 1, 45.

(46) Khan, A. U. *J. Phys. Chem.* **1976**, 80, 2219; Merkel, P. B.; Kearns, D. R. *J. Am. Chem. Soc.* **1972**, 94, 1029.

(42) Graham, D. R.; Marshall, L. E.; Reich, K. A.; Sigman, D. S. *J. Am. Chem. Soc.* **1980**, 102, 5419; Johnson, G. R. A.; Nazhat, N. B. *J. Am. Chem. Soc.* **1987**, 109, 1990; Yamamoto, K.; Kawanishi, S. *J. Biol. Chem.* **1989**, 264, 15435; Barron, E. S. G.; De Meio, R. H.; Klemperer, F. J. *Biol. Chem.* **1936**, 112, 625.

DNA Cleavage on Photoexposure at the d–d Band

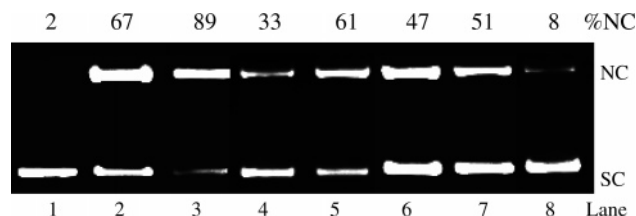


Figure 5. Red-light-induced cleavage of SC pUC19 DNA ($33 \mu\text{M}$) by complexes **1–4** ($80 \mu\text{M}$) in 50 mM Tris-HCl/NaCl buffer (pH 7.2) containing DMF (10%) using a 633 nm CW laser (12 mW) at different exposure times: Lane 1, DNA control (2 h); lane 2, DNA + **1** (1 h); lane 3, DNA + **1** (2 h); lane 4, DNA + **2** (1 h); lane 5, DNA + **2** (2 h); lane 6, DNA + **3** (2 h); lane 7, DNA + **4** (2 h); lane 8, DNA + **1** (in dark).

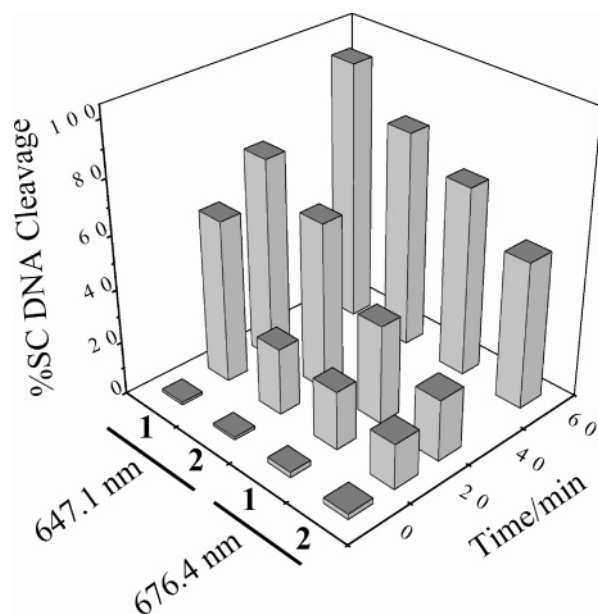


Figure 6. Cleavage of SC pUC19 DNA ($33 \mu\text{M}$) by complexes **1** and **2** ($50 \mu\text{M}$) in 50 mM Tris-HCl/NaCl buffer (pH, 7.2) containing 10% DMF at different photoexposure times using mixed-gas ion laser of wavelengths 647.1 and 676.4 nm (laser power 100 mW). The ligands (HL¹, dpq and dppz) alone exhibit only $\sim 4\%$ and the DNA control shows $\sim 2\%$ cleavage of SC DNA under similar experimental conditions.

All four complexes are cleavage active when irradiated with a CW He–Ne laser (12 mW) of 633 nm , the wavelength known for Photofrin activation (Figure 5 and Figure S7).^{10,47} The cleavage efficiency of the complexes at this laser wavelength follows the same order as observed at 365 nm . We also used a laser wavelength of 647.1 nm to probe the involvement of the long-wavelength d–d band in the photoactivation process for complexes **1** and **2** as they exhibit a d–d band near this wavelength in the absorption spectra (Figures 1 and 6). Both complexes show nicking of supercoiled DNA at this wavelength with a complex concentration of only $50 \mu\text{M}$. Although the ligands individually do not have any visible band in the range of $600\text{--}700 \text{ nm}$ and the ligands alone are inactive in cleaving DNA at red light, the d–d band excitation with 647.1 nm shows significant cleavage of DNA. Photoexcitation of the complexes thus seems to be metal-assisted and involves the metal-based charge transfer and/or d–d transitions resulting in an excited

state followed by an efficient energy transfer to the triplet state that presumably activates oxygen from its stable triplet ($\text{O}_2, {}^3\Sigma_g^-$) to the toxic singlet ($\text{O}_2, {}^1\Delta_g$) state.²⁷ Among the four nucleobases present in DNA, the guanine base is most susceptible for attack by singlet oxygen and guanine oxidation is known to occur for the photoactivation of the PDT drug Photofrin.^{48,49} The present results supplement our previous observation of sulfur-to-copper charge transfer and d–d band involvement in the red-light-induced DNA cleavage by $[\text{Cu}(\text{L}^1)(\text{phen})]^+$.²⁶

We investigated the DNA cleavage activity of complexes **1** and **2** using a laser wavelength of 676.4 nm . Both complexes are found to be photocleavers even at this long wavelength with a complex concentration of $50 \mu\text{M}$ (Figure 6). While complex **1** ($50 \mu\text{M}$) cleaves $97 \pm 2\%$ of the SC pUC19 DNA ($33 \mu\text{M}$) on 1 h photoexposure at 647.1 nm , it shows $71 \pm 2\%$ DNA cleavage at 676.4 nm with the same laser power of 100 mW (Figures S8 and S9). The results unequivocally show the enhanced cleavage activity on photoexcitation at the d–d band. The dpq complex **1** is found to be a significantly better cleaver of DNA in comparison to its phen and dppz analogue due to the presence of the photoactive quinoxaline moiety.²⁷

Conclusions

Two new ternary copper(II) complexes containing NSO-donor Schiff base as photosensitizer and dpq/dppz ligand as DNA binder cum photosensitizer are prepared and their red light-induced DNA cleavage activity studied using CW lasers of different wavelengths. The dpq complex **1** that has been structurally characterized by X-ray crystallography shows significant DNA cleavage activity at red light. To elucidate the photoactivity of the NSO-donor Schiff base, two more complexes containing only dpq/dppz as photosensitizer and a photoinactive ONO-donor Schiff base ligand were prepared and characterized. All complexes exhibit efficient binding to CT-DNA and “chemical nuclease” activity in the presence of 3-mercaptopropionic acid. Complexes **1–4** show cleavage of supercoiled DNA on photoexcitation at 365 nm involving formation of singlet oxygen as the reactive species. Complexes **1** and **2** with two photoactive ligands are better DNA photocleavers than their ONO-donor Schiff base analogues having only one photoactive ligand in the ternary structure. The results that show DNA cleavage on d–d band excitation at red light involving a metal-centered visible band are in complete agreement with our previous report²⁶ of metal-assisted DNA photocleavage using analogous phen complex $[\text{CuL}^1(\text{phen})]^+$.

Acknowledgment. We thank the Department of Science and Technology, Government of India, for financial support (SR/S1/IC-10/2004) and for the CCD facility. We are grateful to the Alexander von Humboldt Foundation for an electrochemical system and the Convener Bioinformatics Center of our Institute for database search.

(47) Ackroyd, R.; Kelty, C.; Brown, N.; Reed, M. *Photochem. Photobiol.* **2001**, *74*, 656. Henderson, B. W.; Dougherty, T. J. *Photochem. Photobiol.* **1992**, *55*, 145.

(48) Carter, P. J.; Breiner, K. M.; Thorp, H. H. *Biochemistry* **1998**, *37*, 13736.

(49) Croke, D. T.; Perrouault, L.; Sari, M. A.; Battioni, J. P.; Mansuy, D.; Hélène, C.; Le Doan, T. *J. Photochem. Photobiol., B* **1993**, *18*, 41.

Supporting Information Available: Cyclic voltammogram of complex **1** (Figure S1), unit cell packing diagram for complex **1** (Figure S2), emission spectral plot (Figure S3), DNA binding by absorption spectral method (Figure S4), and gel electrophoresis diagrams [chemical nuclease activity (Figure S5) and photoinduced DNA cleavage activity at 365 (Figure S6), 633 (Figure S7), 647.1

(Figure S8), and 676.4 nm (Figure S9)], and tables listing full crystallographic data, atomic coordinates, complete bond distances and angles, anisotropic thermal parameters, and hydrogen-atom coordinates for complex **1** (CIF). This material is available free of charge via Internet at <http://pubs.acs.org>.

IC060328E